




RESEARCH ARTICLE | JANUARY 16 2019

Operando study of Pd(100) surface during CO oxidation using ambient pressure x-ray photoemission spectroscopy

Youngseok Yu ; Dongwoo Kim; Hojoon Lim; Geonhwa Kim; Yoobin E. Koh; Daehyun Kim; Kohei Ueda; Satoru Hiwasa; Kazuhiko Mase; Fabrice Bournel; Jean-Jacques Gallet; François Rochet; Ethan J. Crumlin; Philip N. Ross, Jr.; Hiroshi Kondoh ; Do Young Noh; Bongjin Simon Mun 



AIP Advances 9, 015314 (2019)

<https://doi.org/10.1063/1.5081066>

 CHORUS



AIP Advances

Why Publish With Us?



19 DAYS
average time
to 1st decision



500+ VIEWS
per article (average)



INCLUSIVE
scope

[Learn More](#)

Operando study of Pd(100) surface during CO oxidation using ambient pressure x-ray photoemission spectroscopy

Cite as: AIP Advances 9, 015314 (2019); doi: 10.1063/1.5081066

Submitted: 13 November 2018 • Accepted: 4 January 2019 •

Published Online: 16 January 2019



Youngseok Yu,¹ Dongwoo Kim,¹ Hojoon Lim,¹ Geonhwa Kim,¹ Yoobin E. Koh,¹ Daehyun Kim,² Kohei Ueda,² Satoru Hiwasa,² Kazuhiko Mase,³ Fabrice Bournel,^{4,5} Jean-Jacques Gallet,^{4,5} François Rochet,^{4,5} Ethan J. Crumlin,⁶ Philip N. Ross, Jr.,⁶ Hiroshi Kondoh,² Do Young Noh,¹ and Bongjin Simon Mun^{1,a)}

AFFILIATIONS

¹Department of Physics and Photon Science, Gwangju Institute of Science and Technology, Gwangju 61005, Republic of Korea

²Department of Chemistry, Keio University, 3-14-1 Hiyoshi, Kohoku-ku, Yokohama, Kanagawa 223-8522, Japan

³Institute of Materials Structure Science, High Energy Accelerator Research Organization, 1-1 Oho, Tsukuba 305-0801, Japan

⁴Sorbonne Université, CNRS, Laboratoire de Chimie Physique Matière et Rayonnement – Campus Pierre et Marie Curie, F-75005 Paris, France

⁵Synchrotron SOLEIL, L'Orme des Merisiers, Saint-Aubin, F-91192 Gif-sur-Yvette, France

⁶Advanced Light Source, Lawrence Berkeley National Laboratory, Berkeley, California 94720, USA

^{a)}Corresponding author: bsmun@gist.ac.kr

ABSTRACT

The surface chemical states of Pd(100) during CO oxidation were investigated using ambient pressure x-ray photoelectron spectroscopy and mass spectroscopy. Under the reactant ratio of CO/O₂ = 0.1, i.e. an oxygen-rich reaction condition, the formation of surface oxides was observed with the onset of CO oxidation reaction at T = 525 K. As the reactant ratio (CO/O₂) increased from 0.1 to 1.0, ~ 90 % surface oxides remains on surface during the reaction. Upon the formation of surface oxides, the core level shift of oxygen gas phase peak was observed, indicating that change of surface work function. As CO oxidation takes places, i.e. making a transition from CO covered surface to the oxidic surface, the work functions of surface oxide on Pd(100) and Pt(110) display opposite behavior.

© 2019 Author(s). All article content, except where otherwise noted, is licensed under a Creative Commons Attribution (CC BY) license (<http://creativecommons.org/licenses/by/4.0/>). <https://doi.org/10.1063/1.5081066>

INTRODUCTION

The correlation between surface oxides and its catalytic reactivity has been continuously investigated for many years as practical catalysts under reaction conditions exhibit apparent both surface structural modification and oxidation.¹ With the development of numerous innovative *in situ operando* surface science tools, such as polarization modulation infrared reflection absorption spectroscopy (PM-IRRAS),² high-pressure scanning tunneling microscopy (HP-STM),³ surface X-ray diffraction (SXRD),⁴ and ambient

pressure X-ray photoelectron spectroscopy (AP-XPS),⁵ the formation/characteristics of surface oxides under reaction conditions, e.g. high temperature and pressure have been clearly disclosed. In many of these studies, CO oxidation reaction has been employed as it involves standard heterogeneous reaction mechanisms, e.g. molecular adsorption/desorption of reactants, dissociative adsorption of a reactant, and surface reaction. While many of the *in situ operando* techniques have delivered countless valuable information on the surface oxides under close-to-real CO oxidation reaction condition, e.g. the roles of oxide steps, the dynamic modes of

surface oxides phase, and the morphology of surface oxide, the understanding of exact roles of surface oxides in the catalytic reactions are still under debates.⁶⁻⁹

Among the *in situ operando* reaction studies, Pd surface has exhibited rich characters under CO reaction condition. Using AP-XPS and density functional theory (DFT) calculation, Toyoshima et al. showed that the formation of surface oxides and the reaction mechanism strongly depended on the orientation of Pd surfaces.¹⁰⁻¹³ Blomberg et al. investigated the surface chemical states and the reactivity on Pd(100) under various reaction condition,⁹ and reached a similar conclusion as Toyoshima et al. By combining AP-XPS and first-principles kinetic Monte Carlo (1p-kMC) calculation, they showed that the surface oxides formed under an oxygen-rich condition, e.g. CO/O₂ = 0.25, while Pd surface remained in a metallic state under the CO-rich condition, e.g. CO/O₂ = 1.0.⁹

In the meantime, Gao et al., utilizing the PM-IRRAS, investigated the CO oxidation reaction on Pd(100) and Pt(110) surfaces and pointed out the importance of CO mass transfer limitation (MTL) for the accurate understanding of surface reaction mechanism.¹⁴ In the MTL, the conversion of reactants is faster than the transport of products away from the catalyst, which inhibits the reactants to reach the surface. By running the reaction under the different ratio of CO/O₂, the group demonstrates the effect of the MTL in both Pd and Pt surfaces and concludes that metallic surface is the catalytically more active surfaces, supporting the well-known Langmuir-Hinshelwood mechanism on Pd and Pt surfaces.¹⁵

One interesting point of their report is that, from the analysis of turn-over-frequency (TOF) behaviors on Pd(100), i.e. surface reaction rate of Pd, the TOF above the reaction temperature starts to drop under a highly oxidizing condition, e.g. the CO/O₂ ratio = 0.2 and below. (The TOF remains constant at the CO/O₂ ratio of 0.5 and above.) On the other hand, the Pt(110) surface maintains constant TOF at the temperature of the onset of reaction and above, in all CO/O₂ ratio. That is, under the highly oxidizing condition, the CO₂ production rate remains constant in the case of Pt(110), but not in Pd(100). To explain this difference, they pointed out the possible formation of catalytically non-reactive 3-dimensional surface oxides on Pd(100) under the oxygen-rich condition at the reaction temperature. However, from the previous result of AP-XPS and *in situ* XRD under the oxygen-rich condition, the formations of 2-dimensional surface oxides are reported on both Pd(100)^{11,16} and Pt(110)^{17,18} surfaces. Formerly, within similar interest, Yu et al. investigated the formation of surface oxides on Pt(110) under various CO/O₂ ratio and reported that the surface oxides changed little while chemisorbed oxygen is being reduced as CO/O₂ ratio increases.¹⁹

In this report, we focus our attention on the surface oxide formation of Pd(100) surface for identifying the difference or resemblance from that of Pt(110) surface. AP-XPS and mass spectroscopy (MS) are employed to monitor the reactivity and surface oxides simultaneously. As the temperature reached reaction temperature under the oxygen-rich condition, i.e. CO/O₂ = 0.1, the clear enhancement of reactivity was observed with the formation of surface oxides on Pd(100). As

the CO/O₂ increases, the surface oxide remains almost the same, which is similar to the case of Pt(110) CO oxidation.¹⁹ At the onset of CO oxidation reaction, the change of surface work function takes place as the surface makes a transition from CO covered surface to oxidic surfaces, which is revealed from the shift of the binding energy position of the gas phase in contact with the surfaces. It turns out that the work function of Pd(100) changes opposite to that of Pt(110) as the surface oxides forms during CO oxidation reaction.

EXPERIMENTS

Experiments were performed at the AP-XPS endstation of beamline 13B at Photon-Factory of KEK, Japan, and TEMPO beamline at Soleil synchrotron, France.^{10,20} The Pd(100) single crystal was provided from Princeton Scientific Corp. and clean surface of Pd was prepared with cycles of high-temperature annealing (T=1000 K) and Ar⁺ ion sputtering process. The well-ordered surface was confirmed by low-energy electron diffraction (LEED). The O₂ and CO gases were introduced into the high-pressure chamber by adjusting UHV metal leak valves. A CO trap was used to avoid any Ni contamination from CO gas cylinder bottle. Pyrolytic boron nitride (PBN) button heater was used to raise the sample temperature and a K-type thermocouple was attached to the side of the sample by spot welding. During the CO oxidation process, the partial pressure of the reactant and gas products was continuously monitored with MS (HIDEN – HAL201) installed at the first stage of the differential pumping system, located between the high-pressure chamber and electron analyzer. XP spectra of the O 1s, Pd 3d, and C 1s core levels were measured with photon energies of 650 eV, 450 eV, and 450 eV, respectively. The total energy resolution of XPS spectra was set to below 0.3 eV. The binding energy positions of entire XP spectra were calibrated to Fermi level of valence bands spectra. The measured XP spectra were de-convoluted by using Gaussian and Doniach-Šunjić line shapes²¹ after subtracting a Shirley background.

RESULTS AND DISCUSSION

Figure 1 shows the results of MS and sample temperature monitored during the CO oxidation reaction. Initially, the CO and O₂ gases were introduced into the high-pressure reaction chamber at 21.8 and 218.2 mTorr, respectively. The ratio of CO to O₂ was 0.1. As temperature (green line) increases, the CO₂ production starts to increase rapidly in region (I). When the surface temperature reached 525 K, a sharp increase in CO₂ production was observed, which is known as a reaction temperature onset. This reaction temperature matches with the reaction temperature reported by Gao et al. for the same reactant ratio of CO/O₂ = 0.1.¹⁴ Upon reaching the reaction temperature, no additional heating power was added, e.g. fixing the input of sample heater power supply. Yet, the sample temperature continuously increased due to the exothermic reaction of CO oxidation. As CO₂ production continues on the surface, the surface temperature reached 533 K, in region (II). One thing to note in region (II) is that

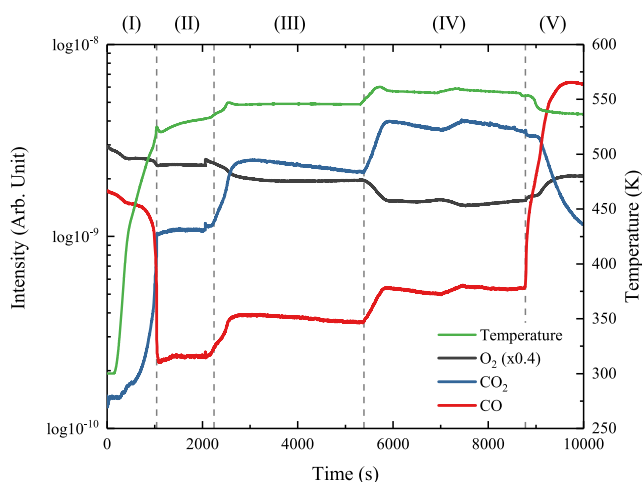


FIG. 1. MS signals as a function of time. The green line refers the temperature of sample, the gray line is the MS intensity of O_2 gas. The red and blue lines are CO gas and CO_2 gas MS intensities, respectively. The MS can be divided into five regions with the Roman numeral at the top of the figure. The region (I) is the low-reactivity region under the ratio of 0.1 and lower temperature than the reaction temperature. The region (II) is high-reactivity region under the ratio of 0.1 and higher temperature than the reaction temperature. The region (III) and (IV) have the ratio of $CO/O_2 = 0.5$ and 1.0, respectively. The region (V) corresponds to the CO/O_2 ratio = 1.5, which shows a low-reactivity region.

the production of CO_2 remained almost constant, which can be explained with MTL process occurring in a high pressure and temperature reaction environment.^{9,14} In MTL process, the reaction rate is determined by the diffusion rate of the minority reactant to the catalysis surface, independent of surface temperature. That is, the CO gas reached the diffusion limiting value at $T = 525$ K and was consumed at a constant rate. To find out the contribution of pressure difference during MTL states, i.e. varying the diffusion rate of CO gas, the CO gas pressure was increased from 21.8 mTorr to 109.1 then 218.2 mTorr while the O_2 gas pressure remained unchanged, i.e. $CO/O_2 = 0.5$ and 1.0, shown in region (III) and (IV), respectively. In both regions of (III) and (IV), the surface temperature arose sharply and reached a stable value. This increase of surface temperature can be explained by the lack of the heat transfer between the gas phase and atmosphere, which occurs during MTL process.²² Also, the CO_2 production slowly starts to decrease afterward. The amount of CO_2 production can be related to that of incoming CO gas to the chamber during MTL process: the CO_2 production increases when CO pressure is increased slightly during region (IV). To inverse the MTL process on the surface, i.e. creating CO-rich reaction condition from the oxygen-rich reaction condition, CO pressure was increased to 327.3 mTorr, shown in region (V), i.e. $CO/O_2 = 1.5$. In region (V), the surface temperature dropped rapidly as the CO_2 production decreased sharply as expected.

Compared to the previous report on Pt(110),¹⁹ the result of Fig. 1 exhibits almost identical trends. As the catalytic reaction occurs, the MTL condition is reached and CO_2 production

follows the profile of CO pressure. That is, the CO oxidation profile on Pd(100) in MS is almost identical to that of Pt(110). To obtain further quantitative information from MS result, a turn-over-frequency (TOF), i.e. the CO_2 formation rate, is calculated with the result of Fig. 1. The details of TOF calculation are described in [supplementary material](#).

Figure 2 shows Arrhenius plots of TOFs of Pd(100) during CO oxidation process at various reactant ratios of CO/O_2 . The calculated TOFs at each CO/O_2 ratio are shown with filled circles, e.g. purple, green, blue, gray circles at $CO/O_2 = 0.1, 0.5, 1.0$, and 1.5, respectively. To compare with previously reported TOFs of CO oxidation on Pd(100) surface under similar conditions, the result of Gao et al.¹⁴ are plotted together in Fig. 2. At $CO/O_2 = 0.1$, the TOFs increases slowly as the temperature increases. At the onset of the reaction temperature at $T = 525$ K, a sudden increase of TOFs is clearly observed. The observed reaction temperature and the degrees of TOFs at $CO/O_2 = 0.1$ show good agreement with the reported value depicted by the red line. In the literature,^{S3-S9} there is some variation on the onset reaction temperature from 450 K ~ 543 K under the oxygen-rich condition, $CO/O_2 = 0.1$, which is most likely due to the experimental geometry of temperature measurement. In our case, the thermocouple is spot welded on the side of the sample. The various values of onset temperature are shown in Table S01, [supplementary material](#).

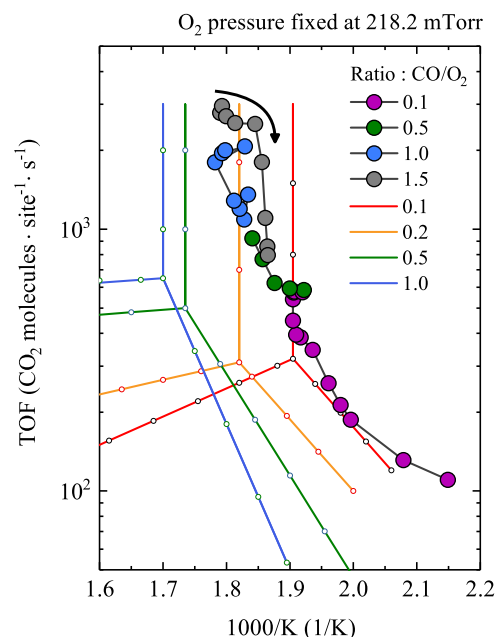


FIG. 2. Arrhenius plots of TOFs of Pd(100) during CO oxidation process at various reactants ratios of CO/O_2 . TOFs is calculated from Fig. 1, which corresponds to solid dots. The solid lines with empty circles are reprinted TOF data of Gao *et al.* with permission from J. Phys. Chem. C **113**, 174 (2009). Copyright 2008 American Chemical Society. Each color represents the difference ratio of CO/O_2 . In the Gao *et al.* experiment, O_2 gas pressure was fixed at 8 Torr. The arrow indicates the track of changed TOFs due to a sudden decrease in reactivity when the CO-rich condition is formed, together with the temperature decrease.

As the CO/O₂ ratio is increased further to 0.5, 1.0, both TOFs and surface temperature continuously increase. Yet, the increasing slope of TOFs is different from the one of CO/O₂ = 0.1, indicating that CO diffusion rate increased. When CO/O₂ ratio becomes 1.5, the TOFs are reduced significantly as CO starts to replace the oxygen adsorption site. As the CO oxidation reaction is monitored with MS, the chemical properties of surface elements were obtained with AP-XPS simultaneously as shown in Fig. 3. The measured spectra were de-convoluted to identify the details of surface chemical states at different CO/O₂ ratios. O 1s spectra were measured at the photon energy of 650 eV while the Pd 3d and C 1s spectra were measured at 450 eV. At these photon energies, the surface sensitivity of XPS measurement is enhanced due to the short inelastic mean free path of photoelectron at a kinetic energy of ~120 eV. Regions (I ~V) in Fig. 3 correspond to the reaction regions shown in Fig. 1.

For region (I), below the reaction temperature under the CO/O₂ ratio of 0.1, gas phases peaks of both O 1s of CO and O₂ were observed, i.e. 536.5 eV for CO gas and 537.3 and 538.4 eV for the doublet of O₂ gas phase, shown in Fig. 3(a) (I). The peak at 531.6 eV corresponds to the CO chemisorption component while the peak at 532.2 eV is associated to the Pd 3p_{3/2} bulk component. The de-convolution of Pd 3d spectrum in region (I) shows three components, one attributed to the Pd bulk element at 335.0 eV, and the other two to CO surface chemisorption states at 335.6 and 336.0 eV which are due to different the number of Pd to CO bonds, as known as p(3√2 × √2)R45°. The CO molecules on the Pd surface can also be identified by C 1s

spectrum at 286 eV, coming from the chemisorption of CO on bridge site. As the CO adsorbed only on the bridge site, a single peak of CO binding energy is expected.

The adsorbed CO molecules on the Pd surface is replaced by adsorbed oxygen as soon as the CO oxidation reaction takes place, as indicated in XP spectra of region (II). The CO-associated components completely disappear from the O 1s, Pd 3d, and C 1s spectra, suggesting the surface makes a transition from CO-covered surface state to an oxygen-covered surface at the onset of CO oxidation reaction. In O 1s spectrum, at the onset of CO oxidation, CO₂ gas phase peak (535.3 eV) starts to emerge with the shift of O₂ gas phase component to higher binding energy. The shift of O₂ gas phase peak, previously witnessed during the similar CO oxidation on Pt(110) experiment with AP-XPS,¹⁹ is understood as the consequence of surface work function change during the reaction.^{5,24} The relation of gas phase peak position and surface work function will be discussed later in detail. In O 1s at region (II), two components appear at the binding energies at 529.2 eV and 530.3 eV, which corresponds to the surface oxide components. As mentioned earlier, the surface oxides are formed under oxygen-rich environment on Pd(100) during CO oxidation reaction. The surface oxide is also identified in the Pd 3d spectra at 335.5 and 336.3 eV. Several groups have already reported the formation of surface oxides on Pd(100) during CO oxidation with in-situ XRD,⁴ in situ STM,⁷ and AP-XPS.¹¹ Toyoshima et al. identified the origin of the surface oxides with DFT calculation and explained the Pd oxide peaks as 2-fold (O 1s at 528.8 eV, Pd 3d at 335.4 eV) and 4-fold oxides (O 1s at

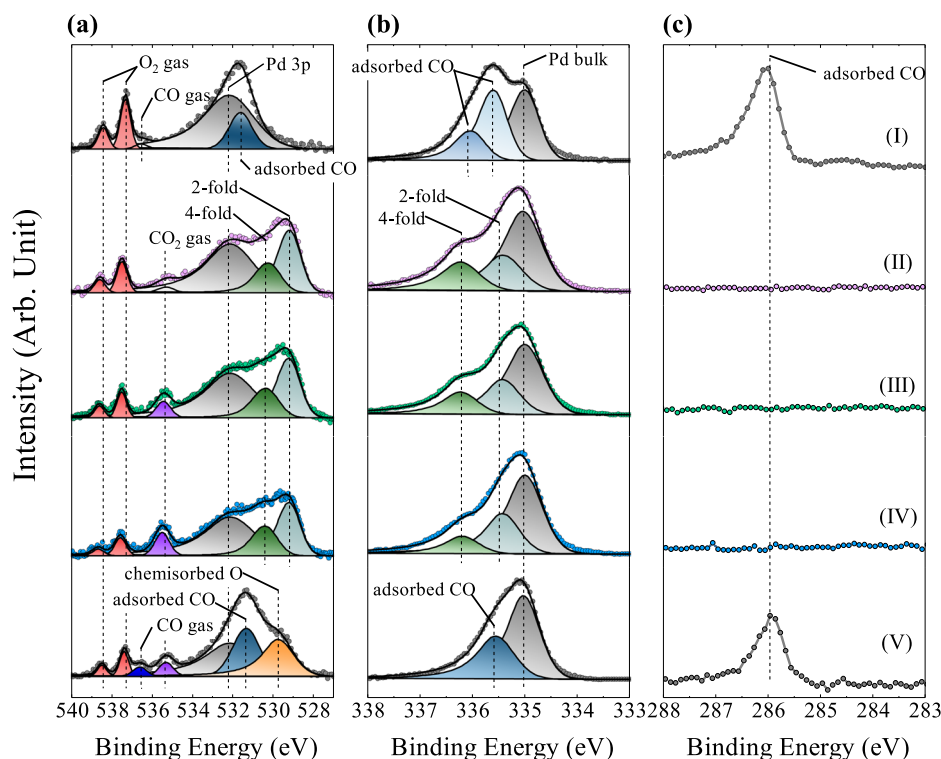


FIG. 3. AP-XP spectra of the (a) O 1s, (b) Pd 3d_{5/2}, (c) C 1s photoemission spectra at each region of Fig. 1 (Regions I to V).

529.6 eV, Pd 3d at 336.2 eV) on a ($\sqrt{5} \times \sqrt{5}$)R27° surface oxide.¹¹ The binding energies of surface oxides in O 1s and Pd 3d in Fig. 3 are in good agreement with previously reported values of surface oxide formed on Pd(100) during CO oxidation.^{9,11}

In region (III) and (IV), under the higher ratio of CO/O₂, e.g. 0.5 and 1.0, the intensity of CO₂ gas phase component starts to increase while that of O₂ gas phase peak reduces, consistent with the result of MS results in Fig. 1. However, no significant changes are found in all other components in O 1s and Pd 3d, and C 1s spectra, including the relative ratio between the 2-fold and 4-fold oxides features. The ratio between the 2-fold and 4-fold oxides to the bulk Pd peak changes only by 10 % while the reactants ratio is increased by 10 times. Previously, the surface oxides formed during CO oxidation experiment on Pt(110) surface also showed the similar behavior as Fig. 3 under the comparable condition of CO/O₂ ratio.¹⁹

As CO/O₂ ratio is further changed to 1.5, the CO gas component starts to appear again as CO₂ gas phase component reduces in region (V) of Fig. 3, indicating a) the presence of CO molecules near the surface, and b) the drop of CO₂ production under a CO-rich environment. As shown in Fig. 1, the CO₂ intensity in the MS profile significantly declines as temperature drops in the region (V). Interestingly, O 1s and Pd 3d show the presence of chemisorbed oxygen at 529.8 eV and 335.5 eV under CO-rich condition. Considering that C 1s spectrum clearly shows the presence of CO on the surface, the spectra of region (V) indicates that both CO and O coexist on the surface. Based on the previous report of the oscillatory behavior of surface oxide during CO oxidation on Pd surface, it is expected that the surface oxide should be removed immediately, recovering metallic surface, upon the end of CO oxidation.⁶ We estimate that the existence of chemisorbed oxygen in region (V) can be understood as the feature of intermediate stage between oxygen-rich condition to a CO-rich condition under CO/O₂ = 1.5 at elevated temperature. At this intermediate stage, the surface makes the transition from rough oxide to a rough metal surface as CO oxidation process ends,⁶ i.e. a surface similar to a polycrystalline surface, and the oxygen species make chemisorption bonding similar to the one of the polycrystalline surface rather than those of on-top and bridge-site in Pd ordered surface. The binding energy of oxygen adsorption in region (V) is similar to that of oxygen chemisorption on Pd polycrystalline surface.²⁵

In order to compare reaction properties of Pd and Pt surface oxides, the spectra of oxygen gas phase are analyzed at CO/O₂ = 0.1 for Pd(100) and CO/O₂ = 0.2 for Pt(110) surface. As mentioned previously, the binding energy position of the gas phase is closely related to the surface work function.²⁴ At the initiation of CO oxidation reaction, the surface oxide is formed immediately, which changes the surface state from CO covered metallic to oxidic. Consequently, the strength of the surface dipole moment, i.e. surface work function, also changes. During AP-XPS measurement, the gas molecules near the surface experience the change of the surface work function during the CO oxidation reaction, resulting in core-level shift of gas phase component.²⁴ In Fig. 4, the intensity maps

of the O 1s spectra on Pd(100) and Pt(110) surfaces, measured during the onset of CO oxidation reaction, are plotted side by side with increasing the surface temperature and TOFs. Fig. 4 shows O 1s oxygen gas phase in the range of 535 ~ 540 eV binding energy and the region (I) and (II) marked on the left-hand side are identical to the regions of Fig. 1. The white circles represent the binding energy position of each spectrum fitted to a Gaussian function. The reaction temperatures on the surface were 525 K and 553 K, which was not significant to make changes in the work function.²⁶

In Fig. 4(a), the shift of O₂ gas phase on the Pd(100) surface is shown. In region (I), the gas phase peak of oxygen, O 1s, is located at 537.13 and 538.23 eV before the reaction. The splitting of O 1s is due to the diamagnetic properties of atomic oxygen. As the surface temperature is increased to the reaction temperature of 525 K, the gas phase of oxygen shifts of 0.28 eV toward higher binding energy side, i.e. 537.41 and 538.51 eV. This change is observed not only under the ratio of CO/O₂ = 0.1 but also under the ratio of CO/O₂ = 1.0.⁹ That is, under the ratio of CO/O₂ = 1.0, the gas phase of oxygen shift is also toward higher binding energy direction. As discussed in detail from the work of Axnanda et al.,²² the binding energy measured from the Fermi level increases with the decrease of surface work function as the gas phase ionization energy (measured from the vacuum level) is constant. From the result of Fig. 3 and 4, we learned that the work function on Pd(100) is reduced with the formation of surface oxide at the onset of CO oxidation.

Interestingly, an identical CO oxidation experiment on Pt(110) surface shows opposite behavior to that of Pd(100). The previous operando study of CO oxidation on Pt(110) using AP-XPS has been re-plotted¹⁹ and the gas phase region of O 1s is shown in Fig. 4(b). To help the comparison, O 1s spectra of before and after reaction regions are plotted in Fig. 4(c) and (d) for Pd(100) and Pt(110) surfaces. The CO oxidation reaction on Pt(110) is carried out with the CO pressure of 40 mTorr and O₂ pressure of 200 mTorr, i.e. oxygen-rich condition with the reactants ratio of CO/O₂ = 0.2. The gas phase of O₂ is seen at 537.86 and 538.96 eV before the reaction. Then, at the onset of CO oxidation, the position of O₂ gas phase shifts to the lower binding energy side by 0.46 eV, i.e. 537.40 eV and 538.50 eV, indicating an increase of the surface work function. It is to note that, as the onset of CO oxidation, the surface of Pt(110) is covered with oxygen species which consists with surface oxide and chemisorbed oxygen.¹⁹

As mentioned in the work of Axnanda et al.,²² as oxygen gas can directly participate in CO oxidation reaction and possibly cause structural changes during CO reaction, a simple comparison of the work function between Pd(100) and Pt(110) may not straightforward. In order to identify the exact value of work function, it is ideal to use non-interacting gas molecules, e.g. Ar, as probing element.²⁴ However, from the result of Fig. 4, we can deduce a qualitative information that the surface work function of Pd(100) decreases as the surface transforms from CO covered surface to oxidic surfaces. In the case of Pt(110), the result is the opposite, i.e. the work function of the oxidic surface is higher than CO-covered surface.

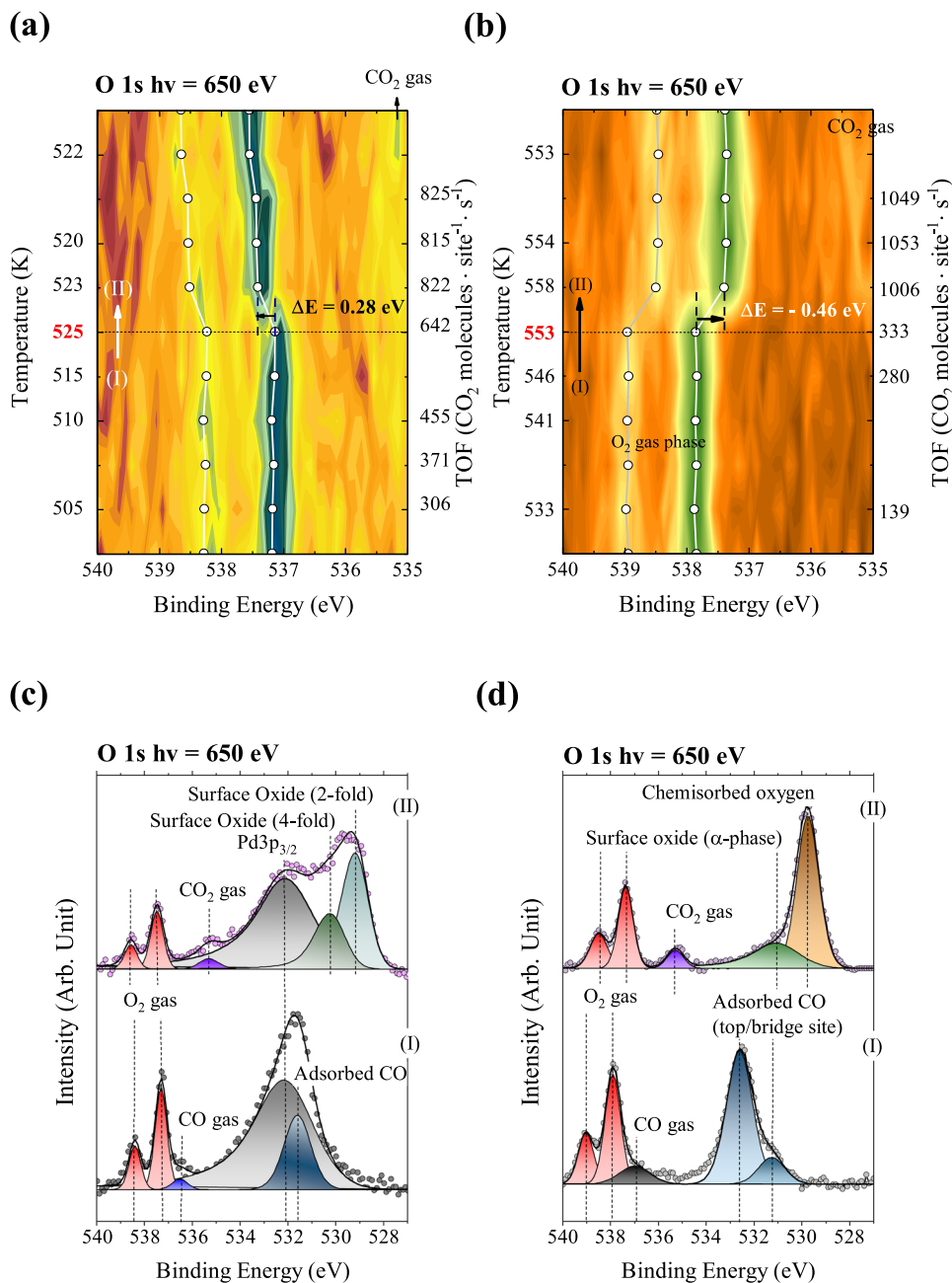


FIG. 4. Sequence plots of O 1s photoemission spectra measured during CO oxidation reaction. Left y-axis shows the sample temperature and right y-axis does TOFs calculated from MS. (a) the trace of oxygen gas phase for Pd(100) under the ratio CO/O₂ = 0.1. (b) Pt(110) under the ratio CO/O₂ = 0.2. (c) AP-XP spectrum of O 1s exhibits the surface chemical states of regions (I) and (II) for Pd(100). (d) Pt(110) of regions (I) and (II). Reprinted with permission from Yu *et al.*, J. Phys.: Condens. Matter **29**, 464001 (2017). Copyright 2017 IOP Publishing.

From the previous theoretical calculation and experimental results, shown in Table I.^{15,27-34} The variation of work function in Fig. 4 agrees well qualitatively with previous findings for Pt(110) surface. In the case of Pt(110), the surface work function increases by 0.6 eV as the surface switches from CO covered to oxidic surfaces.²⁷ However, in the case of Pd(100), the experimental or theoretical value of work function of ($\sqrt{5} \times \sqrt{5}$)R27° Pd(100) surface oxide is not reported yet. Instead, Rogal *et al.* reported the calculated work function values of

PdO surface, e.g. PdO(100)-PdO terminated surfaces.³³ Using their result, the work function of Pd(100) reduces by 0.14 eV as the surface converts from CO covered to PdO(100)-PdO surfaces.³³ As the work function values in Table I are either carried out under UHV condition or calculated, it cannot be directly compared to our results. Yet, the direction of work function change agrees qualitatively with previous findings. In order to obtain the more precise value of work functions on both surfaces under real reaction environments,

TABLE I. Comparison of reported work functions for Pd(100) and Pt(110). All values in eV.

Pt-group	Work Function and its relative shifts upon CO or O adsorption		
	Clean Surface	CO Adsorbed	Oxygen-species
Pd(100)	5.65, 5.8, 5.9 ^a	+ 0.7, + 0.75 ^b	N/A [6.45] ^{c,d}
Pt(110)	5.35 ^e	+ 0.1, + 0.15 ^f	+ 0.8 ^g

^aRef. 28–30.^bRef. 29, 31, and 32.^cThe work function of the ($\sqrt{5}\times\sqrt{5}$)R27° structure is not reported in the previous literatures. The value corresponds to PdO(100)–PdO.^dRef. 33.^eRef. 30, and 34.^fRef. 15, 27, and 31.^gThe work function corresponds to the oxygen covered surface. Ref. 27.

as mentioned above, the AP-XPS measurement with a non-interacting gas can be utilized. Previously, using photoemission electron microscope, Ertl et al.,¹⁵ observed the oscillatory kinetics of surface work function during similar *in situ* reaction condition and argued that the correlation between reactivity and the work function on surface oxides is different between Pd and Pt surfaces, supporting the result of our observation. One important aspect of the result of Fig. 4 is that work function can be monitored by using AP-XPS as the surface reaction occurs.

Lastly, we would like to explain the different properties between Pd(100) and Pt(110) surface oxides under oxygen-rich environment of CO oxidation, observed with PM-IRRAS experiment by Gao et al.¹⁴ From the AP-XPS measurement, no adsorbed CO is observed as the surface oxides forms on Pd(100) surface during the reactants ratio of CO/O₂ = 0.1. On the other hand, PM-IRRAS showed the presence of CO under similar reaction condition. Considering both techniques provide highly surface sensitive information, we estimated that the difference of working pressure range between PM-IRRAS (~ Torr) and AP-XPS (~ mTorr) measurements could generate different surface morphology that results in different behavior of CO adsorption. As Gao et al. suggested, it is certainly possible that 3-dimension surface oxides can be formed under oxygen-rich condition, which can promote the CO adsorption during CO oxidation condition.

CONCLUSION

AP-XPS and MS are employed to investigate the chemical properties of Pd(100) surface during the CO oxidation reaction. As the temperature of surface reaches 525 K under reactant ratio of CO/O₂ = 0.1, the catalytic reaction occurs with formation of surface oxides. In order to find out the contribution of CO pressure during MTL states, the ratio of CO/O₂ is increased from 0.1 to 0.5, and 1.0. The TOF increases together with the CO pressure, and little change is observed on the surface oxides in different reactants ratio. When the CO/O₂ is increased up to 1.5, i.e. CO-rich condition, the CO diffusion rate overcomes the MTL process and the surface oxide disappears, simultaneously. From the shift of oxygen gas phase spectra, the decrease of the surface work function is

observed as Pd(100) surface makes a transition from CO covered surface to oxidic surface at the onset of CO oxidation reaction.

SUPPLEMENTARY MATERIAL

See [supplementary material](#) for “Calculation of TOF”, “Reaction temperature from literatures”, and “OIs state, contour plot”.

ACKNOWLEDGMENTS

This study is supported in part by Basic Science Research Program for support through grants from the National Research Foundation of Korea (NRF) funded by the Korean Government (MOE) (NRF-2015R1A2A2A01004084, NRF-2015K1A3A1A14021261). B. S. Mun would like to acknowledge the supports from SRC (C-AXS, NRF-2015R1A5A1009962) and “GRI (GIST Research Institute)” Project through a grant provided by GIST in 2018. The Advanced Light Source is supported by the Director, Office of Science, Office of Basic Energy Sciences, Materials Science Division, of the U.S. Department of Energy under Contract No. DE-AC02-05CH11231 at Lawrence Berkeley National Laboratory. The AP-XPS experiments were performed under the approval of the Photon Factory Program Advisory Committee (PF PAC-2016G128).

REFERENCES

- ¹H. Over et al., *Science* **287**, 1474 (2000).
- ²F. Gao et al., *Surface Science* **603**, 65 (2009).
- ³B. L. Hendriksen and J. W. Frenken, *Phys. Rev. Lett.* **89**, 046101 (2002).
- ⁴E. Lundgren et al., *Phys. Rev. Lett.* **92**, 046101 (2004).
- ⁵J. Pantförder et al., *Review of Scientific Instruments* **76**, 014102 (2005).
- ⁶B. L. Hendriksen et al., *Nat. Chem.* **2**, 730 (2010).
- ⁷M. Todorova et al., *Surf. Sci.* **541**, 101 (2003).
- ⁸M. J. Hoffmann and K. Reuter, *Top. Catal.* **57**, 159 (2013).
- ⁹S. Blomberg et al., *Phys. Rev. Lett.* **110**, 117601 (2013).
- ¹⁰R. Toyoshima et al., *J. Phys. Chem. C* **116**, 18691 (2012).
- ¹¹R. Toyoshima et al., *J. Phys. Chem. Lett.* **3**, 3182 (2012).
- ¹²R. Toyoshima et al., *J. Phys. Chem. C* **117**, 20617 (2013).
- ¹³H. Kondoh et al., *Catalysis Today* **260**, 14 (2016).

- ¹⁴F. Gao *et al.*, *J. Phys. Chem. C* **113**, 174 (2009).
¹⁵R. Imbihl and G. Ertl, *Chem. Rev.* **95**, 697 (1995).
¹⁶R. van Rijn *et al.*, *Phys. Chem. Chem. Phys.* **13**, 13167 (2011).
¹⁷M. D. Ackermann *et al.*, *Phys. Rev. Lett.* **95**, 255505 (2005).
¹⁸D. R. Butcher *et al.*, *J. Am. Chem. Soc.* **133**, 20319 (2011).
¹⁹Y. Yu *et al.*, *J. Phys.: Condens. Matter* **29**, 464001 (2017).
²⁰SOLEIL, 2018.
²¹S. Doniach and M. Sunjic, *J. Phys. C: Solid State Phys.* **3**, 285 (1970).
²²S. Matera and K. Reuter, *Catal. Lett.* **133**, 156 (2009).
²³J. N. Andersen *et al.*, *Phys. Rev. Lett.* **67**, 2822 (1991).
²⁴S. Axnanda *et al.*, *Nano Lett.* **13**, 6176 (2013).
²⁵K. S. Kim, A. F. Gossmann, and N. Winograd, *Anal. Chem.* **46**, 197 (1974).
²⁶G. Ertl, P. Norton, and J. Rüstig, *Phys. Rev. Lett.* **49**, 177 (1982).
²⁷A. von Oertzen *et al.*, *Journal of Physical Chemistry B* **102**, 4966 (1998).
²⁸K. Christmann and J. E. Demuth, *The Journal of Chemical Physics* **76**, 6308 (1982).
²⁹J. Rogozik, J. Kuppers, and V. Dose, *Surface Science* **148**, L653 (1984).
³⁰N. E. Singh-Miller and N. Marzari, *Physical Review B* **80**, 235407 (2009).
³¹B. Nieuwenhuys, *Surface Science* **105**, 505 (1981).
³²H. Conrad *et al.*, *Surface Science* **43**, 462 (1974).
³³J. Rogal, K. Reuter, and M. Scheffler, *Physical Review B* **69**, 075421 (2004).
³⁴R. Vanselow and X. Q. D. Li, *Surface Science Letters* **264**, L200 (1992).